ELSEVIER

Biochimica et Biophysica Acta 1459 (2000) 422–431

BIOCHIMICA ET BIOPHYSICA ACTA

BBA

www.elsevier.com/locate/bba

Succinate: quinone oxidoreductases: new insights from X-ray crystal structures

C. Roy D. Lancaster [a,*], A. Kröger [b]

[a] *Max-Planck-Institut für Biophysik, Abteilung Molekulare Membranbiologie, Heinrich-Hoffmann-Strasse 7, D-60528 Frankfurt am Main, Germany*

[b] *Johann Wolfgang Goethe-Universität, Institut für Mikrobiologie, Marie-Curie-Strasse 9, D-60439 Frankfurt am Main, Germany*

Received 22 May 2000; accepted 30 May 2000

Abstract

Membrane-bound succinate dehydrogenases (succinate:quinone reductases, SQR) and fumarate reductases (quinol:fumarate reductases, QFR) couple the oxidation of succinate to fumarate to the reduction of quinone to quinol and also catalyse the reverse reaction. SQR (respiratory complex II) is involved in aerobic metabolism as part of the citric acid cycle and of the aerobic respiratory chain. QFR is involved in anaerobic respiration with fumarate as the terminal electron acceptor, and is part of an electron transport chain catalysing the oxidation of various donor substrates by fumarate. QFR and SQR complexes are collectively referred to as succinate:quinone oxidoreductases (EC 1.3.5.1), have very similar compositions and are predicted to share similar structures. The complexes consist of two hydrophilic and one or two hydrophobic, membrane-integrated subunits. The larger hydrophilic subunit A carries covalently bound flavin adenine dinucleotide and subunit B contains three iron-sulphur centres. QFR of *Wolinella succinogenes* and SQR of *Bacillus subtilis* contain only one hydrophobic subunit (C) with two haem *b* groups. In contrast, SQR and QFR of *Escherichia coli* contain two hydrophobic subunits (C and D) which bind either one (SQR) or no haem *b* group (QFR). The structure of *W. succinogenes* QFR has been determined at 2.2 Å resolution by X-ray crystallography (C.R.D. Lancaster, A. Kröger, M. Auer, H. Michel, Nature 402 (1999) 377–385). Based on this structure of the three protein subunits and the arrangement of the six prosthetic groups, a pathway of electron transfer from the quinol-oxidising dihaem cytochrome *b* to the site of fumarate reduction and a mechanism of fumarate reduction was proposed. The *W. succinogenes* QFR structure is different from that of the haem-less QFR of *E. coli*, described at 3.3 Å resolution (T.M. Iverson, C. Luna-Chavez, G. Cecchini, D.C. Rees, Science 284 (1999) 1961–1966), mainly with respect to the structure of the membrane-embedded subunits and the relative orientations of soluble and membrane-embedded subunits. Also, similarities and differences between QFR transmembrane helix IV and transmembrane helix F of bacteriorhodopsin and their implications are discussed.

Keywords: Bioenergetics; Fumarate reductase; Membrane protein; Respiration; Succinate dehydrogenase; X-Ray crystallography

1. Introduction

Succinate:quinone reductase (SQR, EC 1.3.5.1) and quinol:fumarate reductase (QFR) catalyse the two-electron oxidation of succinate to fumarate with concomitant two-electron reduction of quinone

* Corresponding author. http://www.mpibp-frankfurt.mpg.de/lancaster/complexII/index.html;
E-mail: lancaster@mpibp-frankfurt.mpg.de

0005-2728/00/$ – see front matter
PII: S0005-2728(00)00180-8

to hydroquinone (quinol) as well as the reverse reaction. SQR and QFR can be degraded to form succinate dehydrogenase and fumarate reductase (both EC 1.3.99.1), which no longer react with quinone and quinol, respectively. SQRs and QFRs can be divided into three functional subclasses based on the quinone substrate and the in vivo function of the enzyme [1]. *Subclass 1* contains those enzymes which oxidise succinate (E_{M7} = +25 mV [2]) and reduce a high-potential quinone (e.g. ubiquinone (E_{M7} = +90 mV [3]), caldariella quinone (E_{M7} = +103 mV [4])). The SQRs from mammalian mitochondria (respiratory complex II) and many procaryotes belong to this group. *Subclass 2* comprises all those enzymes which catalyse the oxidation of a low-potential quinol (e.g. menaquinol (E_{M7} = −74 mV [5]), rhodoquinol (E_{M7} = −63 mV [6])) and the reduction of fumarate. All QFRs studied so far belong to this subclass. *Subclass 3* includes those enzymes which catalyse the oxidation of succinate and the reduction of a low-potential quinone (e.g. menaquinone, thermoplasma quinone), which is an energetically unfavourable reaction. These subclass 3 enzymes are found in Gram-positive bacteria (e.g. *Bacillus subtilis*, *Paenibacillus macerans*) and archaebacteria (e.g. *Thermoplasma acidophilum*).

SQR and QFR complexes are anchored in the cytoplasmic membranes of archaebacteria, eubacteria and in the inner mitochondrial membrane of eucaryotes with the hydrophilic domain extending into the cytoplasm and the mitochondrial matrix, respectively.

SQR (respiratory complex II) is involved in aerobic metabolism as part of the citric acid cycle and of the aerobic respiratory chain [7]. QFR is involved in anaerobic respiration with fumarate as the terminal electron acceptor [8,9], and is part of the electron transport chain catalysing the oxidation of various donor substrates (e.g. NADH, H_2 or formate) by fumarate. These reactions are coupled via an electrochemical proton potential to ADP phosphorylation with inorganic phosphate by ATP synthase.

Succinate:quinone oxidoreductases generally contain four protein subunits, referred to as A, B, C, and D. Subunits A and B are hydrophilic, whereas the small subunits C and D are integral membrane proteins. Most of the SQRs of Gram-positive bacteria and the QFRs from ε-proteobacteria contain only one larger hydrophobic polypeptide (C), which is thought to have evolved from a fusion of the genes for the two smaller subunits C and D [10–12].

Based on their hydrophobic domain and haem content, succinate:quinone oxidoreductases can be classified in five types, according to Hägerhäll and Hederstedt [10] and recently updated by Hederstedt [11]. Type A enzymes contain two hydrophobic subunits and two haem groups, e.g. SQR from the archaea *Archaeoglobus fulgidus*, *Natronomonas pharaonis*, and *T. acidophilum*. Type B enzymes contain one hydrophobic subunit and two haem groups, as is the case for SQR from the Gram-positive bacteria *B. subtilis*, *P. macerans* and QFR from the ε-proteobacteria *Campylobacter jejuni*, *Helicobacter pylori*, and *Wolinella succinogenes*. Examples for type C enzymes, which possess two hydrophobic subunits and one haem group, are SQR from mammalian mitochondria and from the proteobacteria *Paracoccus denitrificans* and *Escherichia coli* and QFR from the nematode *Ascaris suum*. The QFR of *E. coli* is an example for a type D enzyme, which contains two hydrophobic subunits and no haem group. Finally, type E enzymes, such as SQRs from the archaea *Acidianus ambivalens* and *Sulfolobus acidocaldarius*, but also from the proteobacterium *C. jejuni* and the cyanobacterium *Synechocystis* also contain no haem, but have two hydrophobic subunits very different from the other four types and more similar to those of heterodisulphide reductase from methanogenic archaea [4].

Generally, succinate:quinone oxidoreductases contain three iron-sulphur centres, designated centres 1, 2, and 3, which are exclusively bound by the B subunit. Enzyme types A–D contain one [2Fe-2S], one [4Fe-4S], and one [3Fe-4S] centre as centres 1, 2, and 3, respectively, whereas an additional [4Fe-4S] centre apparently replaces the [3Fe-4S] as centre 3 in the type E enzyme [13]. The A subunit of all described membrane-bound succinate:quinone oxidoreductase complexes contains a covalently bound flavin adenine dinucleotide (FAD) prosthetic group [14]. The chemical structure of the linkage as 8α-[Nε-histidyl]-FAD was first established for mammalian SQR [15] and subsequently for the QFR enzymes of *W. succinogenes* [16] and *E. coli* [17].

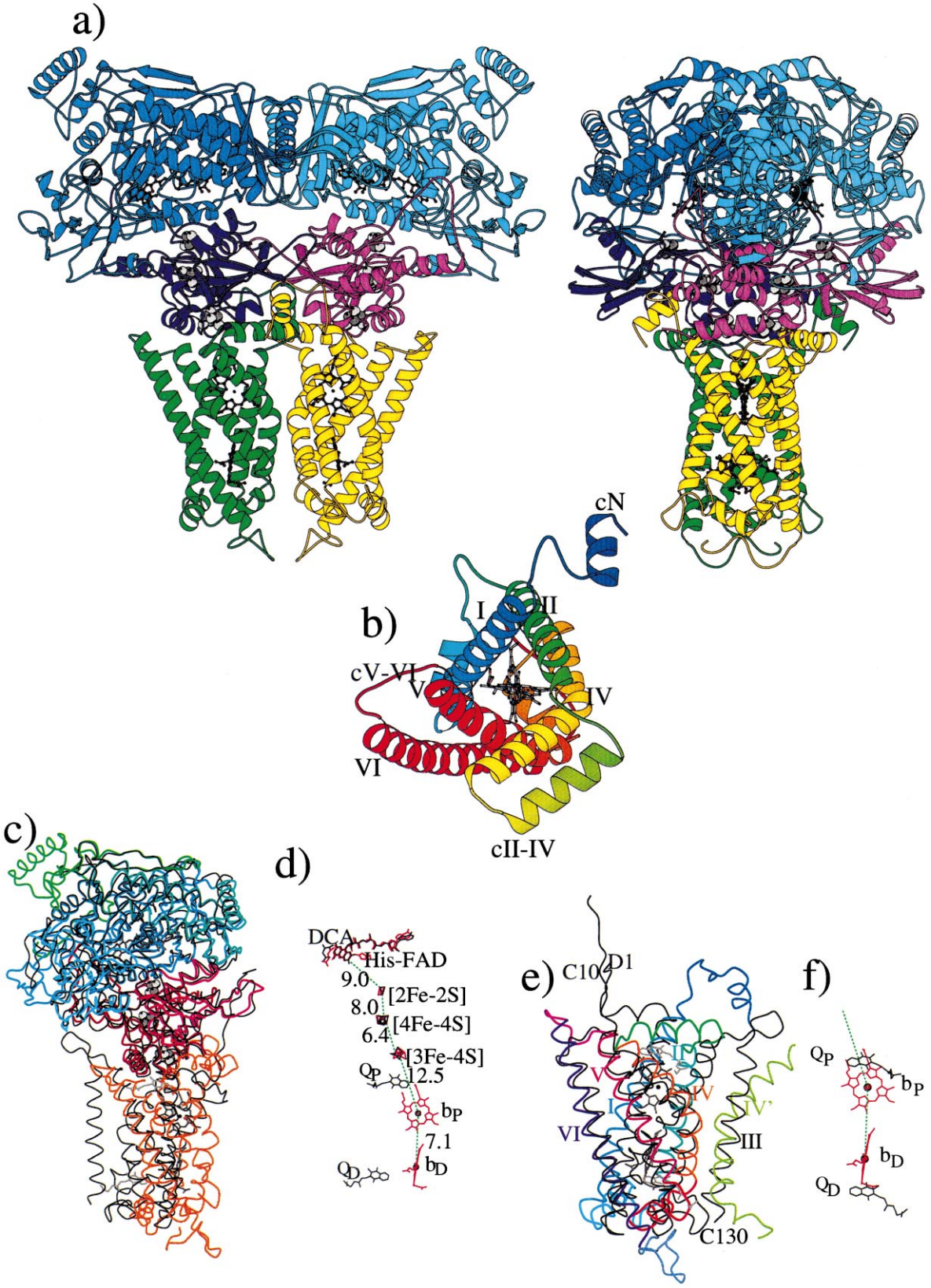
a)
cN
b)
I
II
cV-VI
V
IV
VI
cII-IV
c)
d)
DCA
His-FAD
9.0
[2Fe-2S]
8.0
[4Fe-4S]
6.4
[3Fe-4S]
QP
12.5
bP
7.1
bD
QD
e)
C10
D1
V
I
VI
IV
IV'
III
C130
f)
QP
bP
bD
QD

Fig. 1. (a) Two orthogonal views parallel to the membrane of *W. succinogenes* QFR (PDB entry 1QLA [12]). The polypeptide backbones of the two A subunits are shown in blue and light blue, those of the two B subunits in purple and pink, and those of the membrane-embedded C subunits in green and yellow, respectively. Prepared with the programme MolScript [42]. (b) *W. succinogenes* subunit C as viewed perpendicular to the membrane plane from the cytoplasmic surface. Colour-coded from blue (N-terminus) to red (C-terminus). See text for details on the labelling of the transmembrane helices. This panel and all subsequent panels in this figure and in Fig. 3 were prepared with a version of MolScript [42] modified by Robert Esnouf for colour ramping [43] capabilities. Panels b–f of this figure and Fig. 2 are adapted from [12] with permission. (c–f) Structure of the subunits of *W. succinogenes* QFR (in colour) and comparison to the structure of *E. coli* QFR (in black). The prosthetic groups FAD, haem b_P, and haem b_D of the *W. succinogenes* enzyme are drawn as stick models, the iron-sulphur centres as grey spheres. The quinone models of the *E. coli* enzyme are drawn in grey. Single letters in labels identify the respective subunit. Structures in (c) and (d) are superimposed based on the Cα atoms of the A and B subunits. Structures in (e) and (f) are superimposed based on the Cα atoms of the transmembrane subunits. (c) *W. succinogenes* subunit A domains are drawn in blue (FAD-binding domain), light blue (capping domain), blue-green (helical domain) and green (C-terminal domain) as detailed for panel a. Subunit B domains are drawn in pink ('plant ferredoxin' domain) and brown ('bacterial ferredoxin' domain) as detailed for panel b, subunit C is drawn in orange. (d) Comparison of the electron transfer pathways in the QFR complexes of *W. succinogenes* (red) and *E. coli* (black). Q_P is the 'proximal' quinone, Q_D is the 'distal' quinone. DCA is the dicarboxylate (fumarate in the case of the *W. succinogenes* QFR coordinates (red) and oxaloacetate for the *E. coli* QFR coordinates (black)). Distances between prosthetic groups are 'edge-to-edge' distances in Å as defined in [20]. (e) *W. succinogenes* subunit C consists of five transmembrane helices, two periplasmic and two cytoplasmic helices. The N-terminal cytoplasmic helix (dark blue) is followed by transmembrane helix I (blue), a short periplasmic helix (light blue), transmembrane helix II (blue-green), a second cytoplasmic helix (green), transmembrane helix IV (orange), a second periplasmic helix (red), transmembrane helix V (pink) and transmembrane helix VI (purple). Haem b_P in the top half of the panel and haem b_D in the bottom half of the panel are shown in dark grey. (f) Comparison of the membrane-embedded cofactors in the complexes of *W. succinogenes* (red) and *E. coli* (black). Q_P is the 'proximal' quinone, Q_D is the 'distal' quinone.
←

2. Overall description of the structure

The currently available crystal structures of succinate:quinone oxidoreductases are those of two procaryotic quinol:fumarate reductases. The *E. coli* QFR [18] belongs to the type D enzymes, and the QFR of *W. succinogenes* [12] is of type B. Two structures of the latter enzyme, based on two different crystal forms, are available. Both are considerably better defined and more accurate than the structure of the *E. coli* enzyme. This can be seen from the ratio of the number of independent crystallographic observations to the number of parameters required to define the atomic model (n_{obs}/n_{par}, should be >1), and from the free R value R_T^{free} (should be $<25\%$) as a measure of how accurately the atomic model represents the experimental data. The values for the *W. succinogenes* QFR structures are $n_{obs}/n_{par}=2.31$ and $R_T^{free}=22.4\%$ at 2.2 Å resolution for Protein Data Bank (PDB) entry 1QLA and $n_{obs}/n_{par}=2.02$ and $R_T^{free}=22.3\%$ at 2.33 Å resolution for entry 1QLB. The corresponding values for the *E. coli* QFR structure are $n_{obs}/n_{par}=0.73$ and $R_T^{free}=29.2\%$ at 3.3 Å resolution. Therefore, we will concentrate on *W. succinogenes* QFR for the description of structural features, and those of *E. coli* QFR will be referred to for comparison, as shown in Fig. 1.

In both *W. succinogenes* QFR crystal forms, the two fumarate reductase complexes in the asymmetric unit are associated in an identical fashion, thus forming a dimer (Fig. 1a). As derived from analytical gel filtration experiments, this dimer is apparently also present in the detergent-solubilised state of the enzyme, implying that it is unlikely to be an artifact of crystallisation. Approx. 3665 Å^2 (8%) of the *W. succinogenes* QFR monomer surface is buried upon dimer formation. This is more than 11 times the value of approx. 325 Å^2 reported [18] for the *E. coli* QFR dimer, where the formation of the dimer does seem to be an artifact of crystallisation.

W. succinogenes QFR has an overall length of 120 Å in the direction perpendicular to the membrane. Parallel to the membrane, the maximum width is 130 Å for the dimer, and 70 Å for the monomer. The hydrophobic domain is formed by the menaquinol-oxidising subunit C, which possesses five membrane-spanning helices and binds two haem *b* groups (see Fig. 1b). Attached to subunit C on the cytoplasmic side of the membrane is subunit B, containing the [3Fe-4S], [4Fe-4S], and [2Fe-2S] iron-sulphur centres (in the order of increasing distance from subunit C).

Attached to subunit B, and not in contact with subunit C, is subunit A, which contains the covalently bound FAD and the site of fumarate reduction.

3. Subunit A, the flavoprotein

The Cα traces of the three *W. succinogenes* QFR subunits are shown in Fig. 1c. Subunit A of 73 kDa [19] comprises four domains: a large FAD-binding domain (residues A1–260 and A366–436), a capping domain (A260–366), a helical domain (A436–554) consisting of a single helix and a three-helix bundle, and a C-terminal domain (A554–655), consisting of a pair of antiparallel β-strands followed by a longer and a short helix (see [12] for a more detailed account).

3.1. Binding of fumarate and chemistry of fumarate reduction

The arrangement of residues forming the active site of the oxidised enzyme with fumarate (PDB entry 1QLB [12]) suggests a *trans* hydrogenation mechanism of fumarate reduction as outlined in Fig. 2. The dicarboxylate binding site is mainly formed by the isoalloxazine ring of FAD, two arginine side chains (Arg A301, Arg A404), one histidine side chain (His A369) and the side chain of Phe A141. One carboxylate group of fumarate is bound by polar interactions with Arg A404 and His A369, the other by Arg A301. Tightly bound by hydrogen bonds from both Arg A301 and Arg A404, there is a water molecule, which is also within hydrogen bonding distance of the fumarate α-methenyl C atom. Within hydrogen bonding distance of the fumarate β-methenyl C atom, there is a second water molecule which is also within hydrogen bonding distance to N5 of the FAD isoalloxazine ring and the peptide NH of A48. The side chain Oγ atom of Ser A409 is in a position to form hydrogen bonds with the N1 and O2 atoms of the FAD isoalloxazine ring and the guanidino group of Arg A404. All residues shown in Fig. 2 are widely conserved among succinate:quinone oxidoreductases. Steric constraints and compensating hydrogen bonding interactions force the fumarate out of its planar conformation [12]. Reduction of fumarate could occur by direct hydride transfer [12] or by electron tunnelling [20] from the $FADH_2$ isoalloxazine ring, which is only 2.8 Å away from the fumarate molecule. The latter mechanism is then associated with proton transfer from the N1 of the isoalloxazine ring via Ser A409 and Arg A404 to the fumarate α carbon and a second proton transfer from the N5 of FAD to the fumarate β carbon via the tightly bound water molecule. A slightly different picture is derived from the structures of the soluble single-subunit flavocytochromes c_3 of *Shewanella frigidomarina* [21] and *Shewanella putrefaciens* [22], where the electron density apparently allows the Arg corresponding to Arg A301 to be modelled within hydrogen bonding distance of the fumarate α-methenyl C atom, thus replacing the water molecule in Fig. 2 as the proton donor to the fumarate α carbon.

Release of the product could be facilitated by movement of the capping domain, thus moving the residue Arg A301 away from the dicarboxylate site [12]. This scenario of domain movement has received support from comparing the 'closed' structures of the QFR enzymes with bound dicarboxylate [12,18] to the structures of the single subunit flavoenzymes *E. coli* L-aspartate oxidase (LASPO) [23] and the flavocytochromes of *S. frigidomarina* and *putrefaciens* (see [24] for a review). A feature of LASPO and the flavocytochrome structures lacking bound substrate

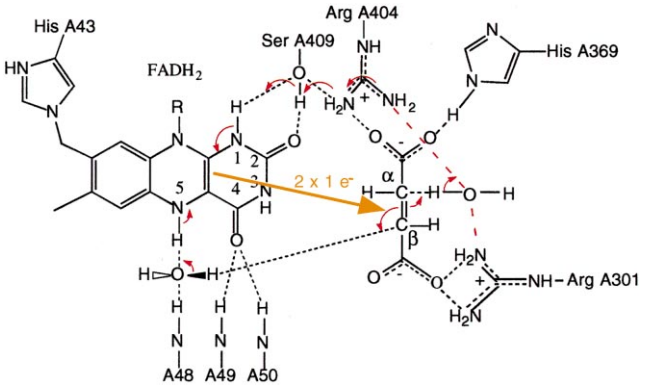

Fig. 2. Possible mechanism of fumarate reduction in *W. succinogenes* QFR involving conserved residues identified in the structure of oxidised QFR in co-complex with fumarate (PDB entry 1QLB [12]). In addition, the peptide backbone NH groups of residues A48–50 are indicated. For clarity, only the isoalloxazine ring portion of $FADH_2$ is shown. Electron tunnelling from the $FADH_2$ isoalloxazine ring system to fumarate is accompanied by proton transfer via two water molecules, thus forming succinate. Modified from [12].

[22,25] is that the capping domain shows mobility by rotating away from the FAD-binding domain.

4. Subunit B, the iron-sulphur protein

The Cα trace of *W. succinogenes* subunit B is shown in Fig. 1c. This subunit of 27 kDa [19] consists of two domains (see Fig. 1c), an N-terminal 'plant ferredoxin' domain (B1–106), binding the [2Fe-2S] iron-sulphur centre and a C-terminal 'bacterial ferredoxin' domain (B106–239) binding the [4Fe-4S] and the [3Fe-4S] iron-sulphur centres.

4.1. Iron-sulphur centres

The [2Fe-2S] iron-sulphur centre is coordinated by the Cys residues B57, B62, B65, and B77 as proposed on the basis of sequence alignments [19]. All four Cys residues are within segments that are in contact with the A subunit. The [4Fe-4S] iron-sulphur centre is ligated to the protein through Cys residues B151, B154, B157, and B218, and the [3Fe-4S] centre is coordinated by Cys residues B161, B208, and B214. The latter three residues are within segments that are in contact with the C subunit.

5. Subunit C, the integral membrane domain

The Cα trace of *W. succinogenes* subunit C is shown in Fig. 1e. This subunit of 30 kDa [26] contains five membrane-spanning segments with preferentially helical secondary structure. These segments are labelled (according to [10]) I (C22–52), II (C77–100), IV (C121–149), V (C169–194), and VI (C202–237). According to the sequence alignment in [10], there is no transmembrane segment III in *W. succinogenes* QFR. To a varying degree, all five transmembrane segments are tilted with respect to the

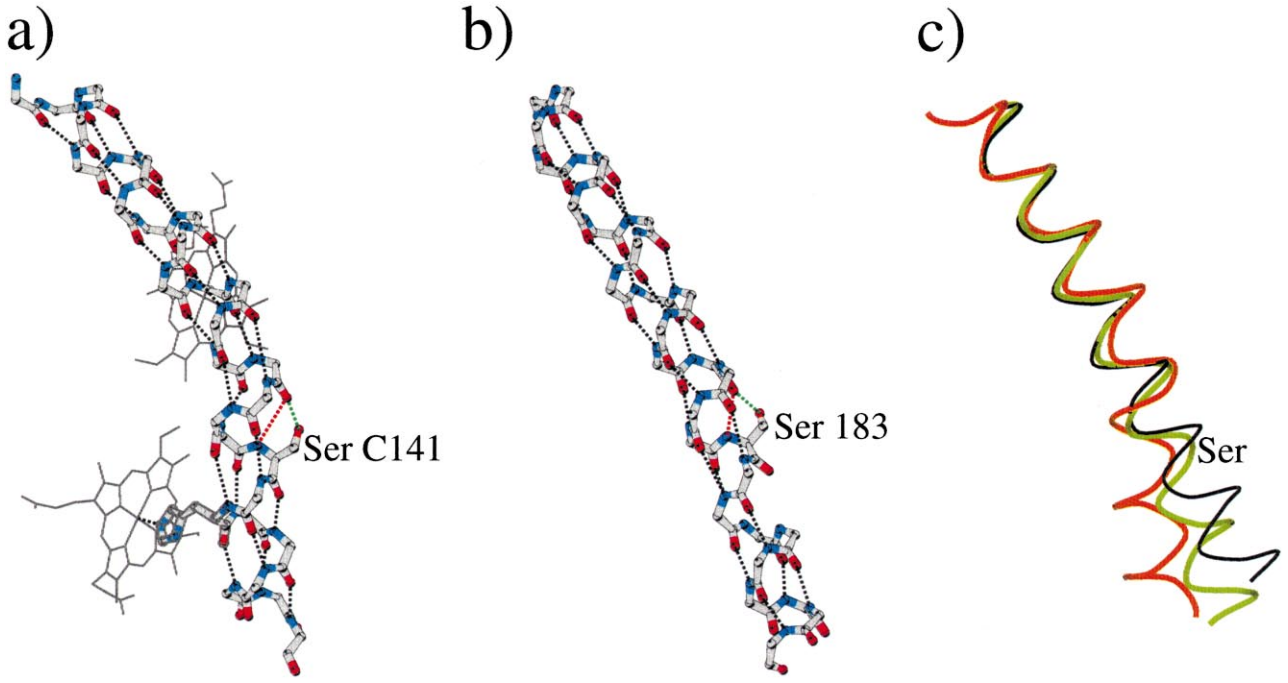

Fig. 3. Comparison of (a) transmembrane helix IV from *W. succinogenes* QFR (PDB entry 1QLA [12]) and (b) transmembrane helix F from *Halobacterium salinarum* bacteriorhodopsin (bR) (PDB entry 1C3W [27]). In both panels hydrogen bonding interactions are indicated by black dashed lines. Highlighted hydrogen bonds donated from the Ser side chain are indicated in green. The corresponding interaction donated by the backbone NH for a standard α-helix is indicated in red. (a) The distance between Ser C141 N and Phe C137 O (indicated in red) is 4.0 Å, the distance between Ser C141 Oγ and Phe C137 O (indicated in green) is 2.8 Å. (b) The distance between Ser 183 N and Val 179 O (red) is 3.0 Å, the distance between Ser 183 Oγ and Val 179 O (green) is 2.6 Å. (c) Superposition of QFR transmembrane helix IV (orange, from panel a), bR transmembrane helix F (green, from panel b) and an idealised α-helix (black).

membrane normal, and helix IV is strongly kinked at position C137. This kink is stabilised by the side chain γ-hydroxyl of Ser C141, which, instead of its backbone NH, donates a hydrogen bond to the carbonyl oxygen of Phe C137 (Fig. 3a). This feature is very similar to that found for helix F of bacteriorhodopsin (bR, PDB entry 1C3W [27], Fig. 3b), part of which tilts during the bR photocycle [28]. Compared to helix IV and an ideal α-helix (Fig. 3c), helix F appears to adopt an intermediate position, also regarding the pattern of hydrogen bonding. It is intriguing to infer a structural change involving helix IV occurring along these lines upon reduction of succinate:quinone oxidoreductases, at least for the dihaem-containing complexes.

When viewed from cytoplasmic side (Fig. 1b), the first four transmembrane segments appear to form a pore-like structure. The 'pore' is blocked by haems b_P and b_D [12]. The membrane-spanning segments are connected by four loops, three of which contain short helices (pI-II: C55–63; cII-IV: C105–118; pIV-V: C158–164). The N-terminus of subunit C is on the cytoplasmic, the C-terminus on the periplasmic side of the membrane. The N-terminal residues C3–11 form a helix denoted 'cN'.

5.1. Relative orientation of soluble and membrane-embedded subunits

As detailed above for the individual soluble subunits, the structure of *E. coli* QFR can be superimposed on the structure of *W. succinogenes* QFR with an r.m.s. deviation of 1.4 Å for 757 Cα atoms from subunits A and B (see Fig. 1c,d). This similarity in structure was expected based on sequence comparisons. However, in this superimposition, the membrane-embedded subunits cannot be aligned. In an alternate superimposition, the transmembrane subunits C and D of the *E. coli* enzyme can be overlayed on to the *W. succinogenes* C subunit with an r.m.s. deviation of 2.25 Å for 113 Cα atoms from the transmembrane helices I, II, IV, V, VI, and from the two periplasmic helices pI-II and pIV-V (see Fig. 1e,f). Compared to the former superimposition, the latter involves a rotation around the membrane normal of approx. 180° and a 25° rotation in the plane of the paper. This immediately leads to two important conclusions [12]. First, the structures of the transmembrane subunits carrying no haems and two haems, respectively, can be aligned to a significant degree, although only eleven of the aligned residues are identical. Second, the relative orientation of the soluble subunits and the transmembrane subunits is different in the QFR complexes from the two species.

5.2. Haem groups

The planes of both haem molecules bound by the *W. succinogenes* enzyme are approximately perpendicular to the membrane surface and their interplanar angle is 95° ([12], see Fig. 1b).

The axial ligands to the 'proximal' haem b_P are His C93 of transmembrane segment II and His C182 of transmembrane segment V. This causes haem b_P to be located towards the cytoplasmic surface of the membrane, and thus towards the [3Fe-4S] iron-sulphur centre. Hydrogen bonds and salt bridges with the propionate groups of haem b_P are formed with the side chains of residues Gln C30, Ser C31, Lys C100, Trp C126 and Lys C193 [12]. Thus, side chains from the residues of all four transmembrane segments forming the 'pore' described above are involved in the binding of haem b_P, which underscores the structural importance of the bound haem [29]. The axial ligands to the 'distal' haem b_D are His C44 of transmembrane segment I and His C143 of transmembrane segment IV, demonstrating that all four haem axial ligands had been correctly predicted by sequence alignment [26] and site-directed mutagenesis [29].

The binding of the two haem *b* molecules described here is very different from that described for the cytochrome bc_1 complex.[30] In *W. succinogenes* QFR, the axial ligands for haem binding are located on four different transmembrane segments. In the cytochrome bc_1 complex, only two transmembrane segments are involved, each providing two axial haem *b* ligands. One consequence of this difference is that the distance between the two haem iron centres is distinctly shorter in QFR (15.6 Å) than it is in the cytochrome bc_1 complex (21 Å).

6. Electron transfer

For the function of QFR, electrons have to be

transferred from the quinol-oxidising site in the membrane to the fumarate-reducing site, protruding approx. 40 Å into the cytoplasm. For *W. succinogenes* QFR, the experimental data [31] are consistent with this electron transfer from the quinol to fumarate occurring via (at least) one haem *b* group. The shortest distance between haem b_P and haem b_D is 4.2 Å. This distance strongly suggests a role in electron transfer for both haem *b* groups. In the event of transmembrane electron transfer *via* the haems, electrogenic proton transfer is possible (see below).

The arrangement of the prosthetic groups in QFR is displayed in Fig. 1d. The fumarate molecule is in van der Waals contact with the isoalloxazine ring of FAD. The connectivity pattern shown in Fig. 1d therefore provides one straightforward possible pathway by which electrons could be transferred efficiently from the dihaem cytochrome *b* to the dicarboxylate binding site.

The redox midpoint potentials of the iron-sulphur centres [31] follow the order high (−24 mV)-low (< −250 mV)-high (−59 mV) with increasing proximity to the covalently bound FAD. The midpoint potentials reported for all three iron-sulphur centres are higher than the upper end of the range normally found [32] for [2Fe-2S] centres in [2Fe-2S] ferredoxins (−220 mV to −420mV), [4Fe-4S] centres in [7Fe-8S] ferredoxins (−380 mV to −650mV) and [3Fe-4S] centres in [7Fe-8S] ferredoxins (−120 mV to −450mV), respectively. The main reason for the higher midpoint potentials compared to the respective soluble ferredoxins appears to be the buried nature of subunit B and its prosthetic groups [12], thus stabilising the reduced, lesser charged forms of the iron-sulphur centres.

The [4Fe-4S] iron-sulphur centre has a very low potential ($E_m < -250$ mV) and has been suggested not to participate in electron transfer (see [1] for a review). However, the determined low potential may be an artefact due to anti-co-operative electrostatic interactions between the redox centres [33]. The position of the [4Fe-4S] centre as revealed in the structures of *W. succinogenes* QFR and *E. coli* QFR is highly suggestive of its direct role in electron transfer from the [3Fe-4S] centre to the [2Fe-2S] centre. Despite this major thermodynamically unfavourable step, the calculated rate of electron transfer is on a microsecond scale, demonstrating that this barrier can easily be overcome by thermal activation as long as the electron transfer chain components are sufficiently close to promote intrinsically rapid electron tunnelling [34].

The prosthetic groups of *W. succinogenes* QFR are compared to those of the *E. coli* enzyme based on the superposition of the soluble subunits (Fig. 1d) and the superposition of the membrane-embedded subunits (Fig. 1f). Correlated with the similarity in structure of the soluble protein subunits (see Fig. 1c), the histidyl-FAD group and the three iron-sulphur centres superimpose well, with the exception of those [3Fe-4S] sulphur atoms which are oriented towards the membrane-embedded subunit(s).

6.1. Quinone binding sites

The existence of up to three quinone-binding sites in succinate:quinone oxidoreductases is being discussed (reviewed in [1,2]): a 'proximal' binding site, close to haem b_P (where present) and the [3Fe-4S] iron-sulphur centre, and a 'distal' binding site close to haem b_D. In some cases, the 'proximal' binding site has been reported to contain an EPR-detectable semiquinone pair. Unfortunately, no density for a quinone could be found in either crystal form of the oxidised *W. succinogenes* QFR. In analogy to the cytochrome bc_1 complex [30], the quinone binding site(s) is (are) expected to be located in the vicinity of haem b_P or (and) haem b_D. In analogy to the photosynthetic reaction centre (see [35] for a review), the quinone(s) is (are) expected to bind in the vicinity of the Trp 'belts' in the hydrophobic surface-to-polar transition zone of the membrane [12].

The *E. coli* QFR coordinate set 1FUM [18] contains models for two quinone molecules per ABCD monomer. Although some of the atomic temperature factors of the quinone ring atoms are larger than 100 $Å^2$, indicating that these quinone models may not be well defined, these models have been included in Fig. 1b,f for comparison. In the superposition of the transmembrane subunits (Fig. 1f), the *E. coli* proximal quinone model clashes with the *W. succinogenes* ring A haem b_P propionate. The distal *E. coli* quinone model clashes with the ring A haem b_D propionate. In summary, this superposition indicates that the quinone binding site(s) of the *W. succinogenes* enzyme cannot simply be derived from superimposi-

tion with the *E. coli* QFR coordinates. In addition, it questions whether the *E. coli* Q_p model is relevant for those succinate quinone oxidoreductases that contain a proximal haem group.

An overview of the different possibilities of electron and proton transfer in succinate:quinone oxidoreductases is shown in Fig. 4. In mitochondrial complex II and other C-type enzymes, such as SQR from *P. denitrificans* and *E. coli*, electron transfer from succinate to ubiquinone does not lead to the generation of a transmembrane electrochemical potential (see [2] for a review), since the protons released by succinate oxidation are on the same side of the membrane as those consumed in association with quinone reduction (Fig. 4a). The emerging picture [36] regarding the succinate:menaquinone reductases from Gram-positive bacteria, type B enzymes, is that the thermodynamically unfavourable coupling of succinate oxidation and menaquinone reduction involves a distal quinone reduction site and is driven by the transmembrane electrochemical potential (Fig. 4b).

It is unlikely that transmembrane electron transfer occurs in the *E. coli* QFR, because of the large edge-to-edge distance of approx. 25 Å between the two quinone models [12,24]. Therefore, it is most likely that quinol oxidation occurs at a proximal site, which is also a possibility for the *W. succinogenes* QFR ([37], Fig. 4c). The close proximity between the two haems of *W. succinogenes* QFR as described above, however, offers a much more straightforward possibility for transmembrane electron transfer. In the presence of a distal menaquinol-oxidising site (Fig. 4d), releasing two protons into the periplasm per oxidised quinol, in combination with transmembrane electron transfer via the two haems in *W. succinogenes* QFR, and the binding of two protons from the cytoplasm per reduced fumarate would lead to the generation of a transmembrane electrochemical potential [2,12,24]. This would be the analogous reaction to that discussed for the SQR of Gram-positive bacteria (Fig. 4b), but in the opposite direction [2].

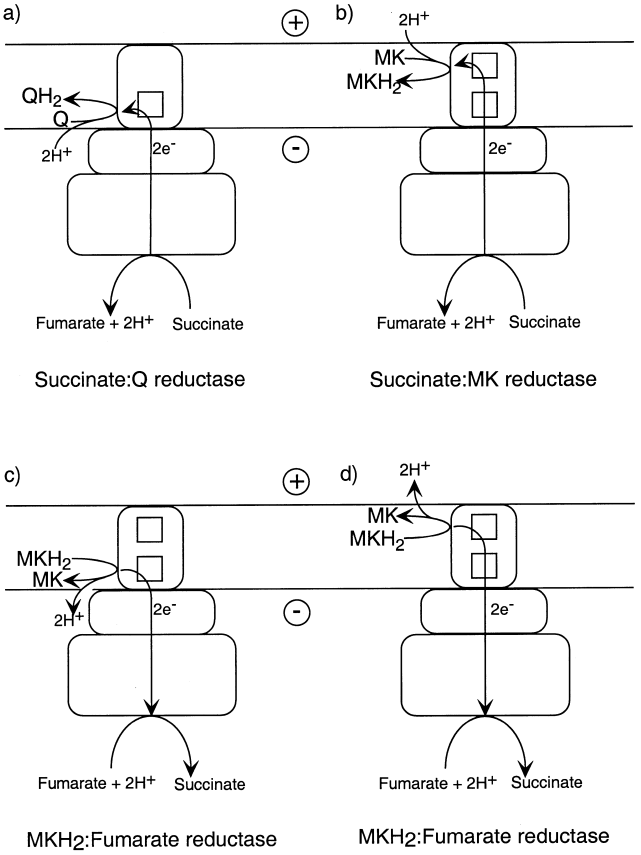

Fig. 4. Electron flow in aerobic respiration (a,b) and anaerobic respiration (c,d), respectively, and the possible utilisation (b) and generation (d) of a transmembrane electrochemical potential. In bacteria, the negative side is the cytoplasm, the positive side the periplasm. For mitochondrial systems, these are the mitochondrial matrix and the intermembrane space, respectively.

7. Medical aspects

In higher organisms, mutations of succinate:quinone reductase have been linked to oxidative stress and aging in nematodes [38] and to leukodystrophy with Leigh syndrome in humans ([39]; see [40] for a review of other human complex II deficiencies). While the former mutation is localised in the gene for the C subunit, the latter was localised in the gene for the A subunit, as is another potentially lethal mutation in humans, Arg A450→Cys [24]. This residue corresponds to A404 in *W. succinogenes* QFR and is not only important for catalysis (see Fig. 2) but also for stabilising the intermediate during covalent attachment of FAD [41]. Consequently, the mutated complex contains non-covalent FAD and neither oxidises succinate nor reduces fumarate [24]. Patients survive because they have a second allele producing normal subunit A [24].

Acknowledgements

CRDL is grateful to H. Michel for support. We thank A. Roth for help in preparing Fig. 4, and J. Simon and R. Groß for discussions. We gratefully acknowledge support by DFG Sonderforschungsbereich 472 ('Molecular Bioenergetics', P5 (AK) and P19 (CRDL)).

References

[1] C. Hägerhäll, Biochim. Biophys. Acta 1320 (1997) 107–141.
[2] T. Ohnishi, C.C. Moser, C.C. Page, P.L. Dutton, T. Yano, Structure 8 (2000) R23–R32.
[3] H. Ding, C.C. Moser, D.E. Robertson, M.K. Tokito, F. Daldal, P.L. Dutton, Biochemistry 34 (1995) 15979–15996.
[4] G. Schäfer, M. Engelhard, V. Müller, Microbiol. Mol. Biol. Rev. 63 (1999) 570–620.
[5] R.K. Thauer, K. Jungermann, K. Decker, Bacteriol. Rev. 41 (1977) 100–180.
[6] F. Saruta, T. Kuramochi, K. Nakamura, S. Takamiya, Y. Yu, T. Aoki, K. Sekimizu, S. Kojima, K. Kita, J. Biol. Chem. 270 (1995) 928–932.
[7] M. Saraste, Science 283 (1999) 1488–1493.
[8] A. Kröger, Biochim. Biophys. Acta 505 (1978) 129–145.
[9] A. Kröger, V. Geisler, E. Lemma, F. Theis, R. Lenger, Arch. Microbiol. 158 (1992) 311–314.
[10] C. Hägerhäll, L. Hederstedt, FEBS Lett. 389 (1996) 25–31.
[11] L. Hederstedt, Science 284 (1999) 1941–1942.
[12] C.R.D. Lancaster, A. Kröger, M. Auer, H. Michel, Nature 402 (1999) 377–385.
[13] C.M. Gomes, R.S. Lemos, M. Teixeira, A. Kletzin, H. Huber, K.O. Stetter, G. Schäfer, S. Anemüller, Biochim. Biophys. Acta 1411 (1999) 134–141.
[14] T.P. Singer, W.S. McIntire, Methods Enzymol. 106 (1984) 369–378.
[15] W.H. Walker, T.P. Singer, J. Biol. Chem. 245 (1970) 4224–4225.
[16] W.C. Kenny, A. Kröger, FEBS Lett. 73 (1977) 239–243.
[17] J.H. Weiner, P. Dickie, J. Biol. Chem. 254 (1979) 8590–8593.
[18] T.M. Iverson, C. Luna-Chavez, G. Cecchini, D.C. Rees, Science 284 (1999) 1961–1966.
[19] F. Lauterbach, C. Koertner, S.P. Albracht, G. Unden, A. Kroeger, Arch. Microbiol. 154 (1990) 386–393.
[20] C.C. Page, C.C. Moser, X. Chen, P.L. Dutton, Nature 402 (1999) 47–52.
[21] P. Taylor, S.L. Pealing, G.R. Read, S.K. Chapman, M.D. Walkinshaw, Nat. Struct. Biol. 6 (1999) 1108–1112.
[22] D. Leys, A.S. Tsapin, K.H. Nealson, T.E. Meyer, M.A. Cusanovich, J.J. van Beeumen, Nat. Struct. Biol. 6 (1999) 1113–1117.
[23] A. Mattevi, G. Tedeschi, L. Bacchella, A. Coda, A. Negri, S. Ronchi, Structure 7 (1999) 745–756.
[24] B.A.C. Ackrell, FEBS Lett. 466 (2000) 1–5.
[25] V. Bamford, P.S. Dobbin, D.J. Richardson, A.M. Hemmings, Nat. Struct. Biol. 6 (1999) 1104–1107.
[26] C. Körtner, F. Lauterbach, D. Tripier, G. Unden, A. Kroeger, Mol. Microbiol. 4 (1990) 855–860.
[27] H. Luecke, B. Schobert, H.T. Richter, J.-P. Cartailler, J.K. Lanyi, J. Mol. Biol. 291 (1999) 899–911.
[28] J. Vonck, Biochemistry 35 (1996) 5870–5878.
[29] J. Simon, R. Gross, M. Ringel, E. Schmidt, A. Kröger, Eur. J. Biochem. 251 (1998) 418–426.
[30] D. Xia, C.A. Yu, H. Kim, J.Z. Xian, A.M. Kachurin, L. Zhang, L. Yu, J. Deisenhofer, Science 277 (1997) 60–66.
[31] G. Unden, S.P.J. Albracht, A. Kröger, Biochim. Biophys. Acta 767 (1984) 460–469.
[32] H. Beinert, J. Biol. Inorg. Chem. 5 (2000) 2–15.
[33] J.C. Salerno, Biochem. Soc. Trans. 19 (1991) 599–605.
[34] P.L. Dutton, X. Chen, C.C. Page, S. Huang, T. Ohnishi, C.C. Moser, in: G.W. Canters, E. Vijgenboom (Eds.), Biological Electron Transfer Chains: Genetics, Composition and Mode of Operation, Kluwer Academic Publishers, Dordrecht, 1998, pp. 3–8.
[35] C.R.D. Lancaster, Biochem. Soc. Trans. 27 (1999) 591–596.
[36] J. Schirawski, G. Unden, Eur. J. Biochem. 257 (1998) 210–215.
[37] V. Geisler, R. Ullmann, A. Kröger, Biochim. Biophys. Acta 1184 (1994) 219–226.
[38] N. Ishii, M. Fijii, P.S. Hartman, M. Tsuda, K. Yasuda, N. Senoo-Matsuda, S. Yanase, D. Ayusawa, K. Suzuki, Nature 394 (1998) 694–697.
[39] T. Bourgeron, P. Rustin, D. Chretien, M. Birchmachin, M. Bourgeois, E. Viegaspequignot, A. Munnich, A. Rötig, Nat. Genet. 11 (1995) 144–149.
[40] P. Rustin, T. Bourgeron, B. Parfait, D. Chretien, A. Munnich, A. Rötig, Biochim. Biophys. Acta 1361 (1997) 185–197.
[41] M. Mewies, W.S. McIntire, N.S. Scrutton, Protein Sci. 7 (1998) 7–20.
[42] P.J. Kraulis, J. Appl. Crystallogr. 24 (1991) 946–950.
[43] R.M. Esnouf, J. Mol. Graph. Model. 15 (1997) 132–134.